

Characterization and optimization of the detection sensitivity of an atomic force microscope for small cantilevers

Tilman E. Schäffer^{a)} and Paul K. Hansma

Department of Physics, University of California, Santa Barbara, California 93106-9530

(Received 19 February 1998; accepted for publication 24 July 1998)

The detection sensitivity of an atomic force microscope with optical beam deflection for small cantilevers is characterized experimentally and theoretically. An adjustable aperture is used to optimize the detection sensitivity for cantilevers of different length. With the aperture, the signal-to-noise ratio of cantilever deflection measurements is increased by a factor of 1.5 to nearly 3. A theoretical model is set up that generally describes the optical beam deflection detection in an atomic force microscope. This model is based on diffraction theory and includes the particular functional shape of the cantilever. © 1998 American Institute of Physics.

[S0021-8979(98)01021-4]

I. INTRODUCTION

Recently, it has become possible to operate atomic force microscope¹ (AFM) cantilevers smaller than 10 μm in length.^{2,3} Using small cantilevers is one way of addressing the demand of advanced applications^{4,5} for low-noise and high-speed measurements.^{6,7} One of the limiting fundamental noise sources in the AFM is thermal noise of the cantilever. With the use of smaller cantilevers, this noise source can be reduced such that, in principle, very small forces can be measured. With smaller forces, deflections of the cantilever become smaller and detection noise becomes more significant, especially for measurements at dc (force spectroscopy,⁵ molecular sensing,⁸ attractive- and repulsive-force mode imaging⁹). Therefore, it is important to have a good, low-noise detection system. A low-noise detection system is also required in cases where thermal noise is the actual subject of study and not a limiting noise source.¹⁰ The deflections of AFM cantilevers are typically detected with the optical beam deflection method.^{11,12} This method uses angular changes of an optical beam, reflected off the cantilever, to measure the deflection. The advantage of optical beam deflection compared to other detection schemes^{1,13–19} is simplicity. Remote sensing with the optical beam that is focused to a spot on the cantilever and reflected off it physically separates the detector from the cantilever–sample environment. The cantilever can therefore easily be submerged in transparent liquids.²⁰ Various cantilever sizes,^{21,22} shapes^{23,24} and materials^{3,25–27} can be chosen to satisfy particular experimental requirements.

Small cantilevers need small focused spot sizes. To date, focused spot sizes down to 1.6 μm in diameter have been achieved.³ Small focused spot sizes are not always preferable, since detection sensitivity is highest when the focused spot size is matched to the cantilever size.^{28,29} For larger cantilevers, therefore, larger focused spot sizes are best. In order to operate a wide range of cantilever sizes at optimum detection sensitivity, the AFM needs to be capable of adjust-

ing the focused spot size to the particular cantilever size. An easy way of doing this is with an adjustable aperture in the incident beam path. We show in this article that we can significantly increase the signal-to-noise ratio of the detection when using an adjustable aperture. To explain this behavior, we set up a simple theoretical model. This new model is based on diffraction theory that takes into account the functional shape of the cantilever and extends existing theories^{28,29} that approximate the cantilever as a rigid and hinged beam.

II. EXPERIMENT

The measurements were taken on a home-built AFM with optical beam deflection detection. This AFM was designed to produce a small focused spot on the cantilever and can be used to operate small cantilevers.³ A collimated laser beam of wavelength $\lambda=670$ nm and 4 mW power from a single-mode laser diode illuminates a slit aperture of width a (Fig. 1). The light that passes through the aperture forms the incident beam and is focused by a lens system to a spot with an irradiance profile I_c on the cantilever. This focused spot is oriented with its long axis along the cantilever. The center of the focused spot can be moved on the cantilever to a position p_c . The light reflected by the cantilever forms the reflected beam that passes back through the lens. It is separated from the incident beam by the polarizing beamsplitter with the $\lambda/4$ wave plate and is directed onto the photodetector where it illuminates the two segments, A and B , with an irradiance profile I_d . The spot is centered on the detector such that the same power is incident on each segment: $P_A=P_B$. The difference of those powers, P_A-P_B , provides the difference signal of a measurement of the cantilever's deflection.

Pictures of the focused spot on a 40 μm long silicon nitride cantilever similar to ones described before⁷ were taken for different aperture widths, a , using a CCD camera [Figs. 2(a)–2(d)]. At full aperture width ($a=2$ mm), the focused spot on the cantilever is smallest [Fig. 2(a)]. When the aperture width is reduced, the focused spot is reduced in power but becomes larger in size [Fig. 2(b) and 2(c)]. At an

^{a)}Electronic mail: tilman@physics.ucsb.edu

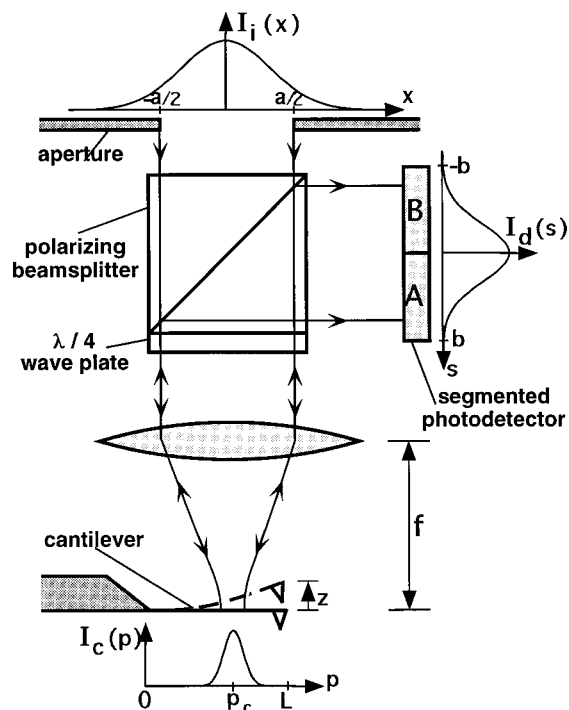


FIG. 1. Schematic of the AFM with optical beam deflection detection. A collimated laser beam illuminates a slit aperture of width a . The light that passes through the aperture forms the incident beam and is focused by the lens to a spot onto the cantilever. The center of this focused spot is moved to position p_c . The light reflected by the cantilever is projected onto the segmented photodetector. A deflection of the cantilever moves the spot on the detector. The polarizing beam splitter and $\lambda/4$ wave plate maximize the fraction of light reflected from the cantilever that reaches the segmented photodetector.

intermediate aperture width ($a=0.19$ mm), the spot approximately fills the cantilever [Fig. 2(c)]. With a further reduction of the aperture width, the spot overfills the cantilever (Fig. 2d) and light is spilled over the cantilever's edges. This effect of increasing spot size with decreasing aperture width can be understood by diffraction theory: The lens creates a diffraction pattern of the aperture in the cantilever plane, thus a large aperture width results in a small spot size and vice versa. In other words, a large incident beam is needed to produce a small spot on the cantilever. A quantitative treatment of the effect of the aperture will be given in Sec. III. Note that the focused spot changes size predominantly in one dimension only, namely in the direction of the cantilever length and not in the direction of the cantilever width, since the slit aperture only restricts the incident beam in that direction.

For measurements of the optical beam deflection detection sensitivity, a $10\ \mu\text{m}$ long cantilever was oscillated in air, far off any surface, at its fundamental vibrational resonance frequency (1.78 MHz) by a piezo actuator. The difference signal of the measurement was the difference of the light power incident on each detector segment, $P_A - P_B$, at maximum cantilever deflection. The difference signal was maximized by moving the center of the focused spot on the cantilever to an optimum position p_c . For large aperture widths (i.e., small focused spot sizes), this optimum position was toward the tip of the cantilever and moved closer toward the

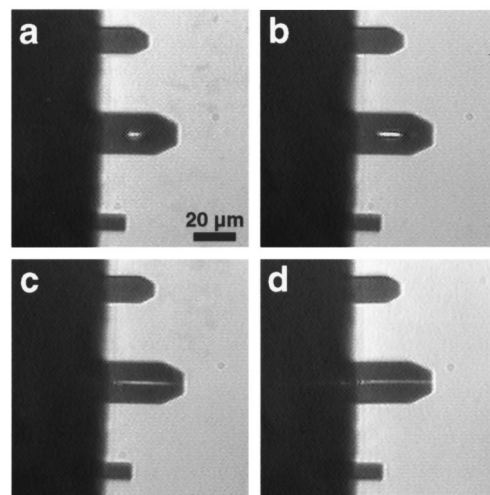


FIG. 2. Focused spot at different aperture widths. A smaller aperture width results in a larger spot size, which affects the optical beam deflection sensitivity. (a) Aperture width $a=2.0$ mm (full aperture). The focused spot is smallest in length. This small focused spot size results in a large spot size at the detector. (b) Aperture width $a=0.52$ mm. Decreasing the aperture width means decreasing the effective numerical aperture of the optical system, thus increasing the focused spot size (even though its power is reduced). (c) Aperture width $a=0.19$ mm. The focused spot approximately fills the cantilever, a condition that theoretically maximizes the signal-to-noise ratio. (d) Aperture width $a=0.10$ mm. The focused spot overfills the cantilever and the signal-to-noise ratio drops. For maximum detection sensitivity, each spot must be moved to its optimum position on the cantilever.

center of the cantilever for decreasing aperture width (i.e., larger focused spot sizes). The difference signal at the respective optimum position of the focused spot on the cantilever is plotted versus the total power incident on the detector (Fig. 3). For large aperture widths, much light power is collected at the detector and the difference signal is high (normalized to 1 at full aperture width). When the aperture width is decreased and less power is collected at the detector, the difference signal at first stays about constant down to a power of about 0.8 a.u. and only decreases with a further reduction of the power. This is different from the behavior of the difference signal when the laser power is reduced by using filters in the incident beam path but the aperture width

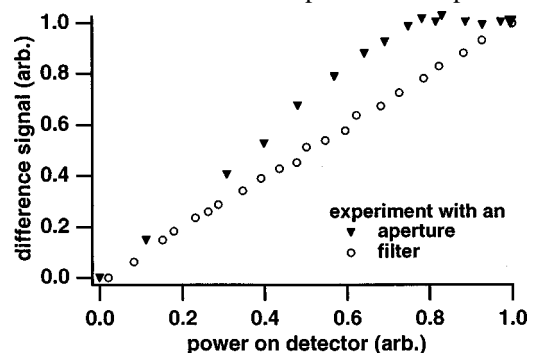


FIG. 3. Detector difference signal as a function of the light power on the detector for two different methods of modifying the incident beam. When a filter is used to lower the power of the incident beam, the difference signal drops inversely proportional to the power. When an aperture is used to narrow the size of the incident beam, the difference signal stays about constant for high powers and decreases for lower powers (smaller aperture widths). Since the focused spot size increases when decreasing the aperture width, the spot was moved on the cantilever for each aperture size to maximize the difference signal (toward the tip for small spots, and toward the center for larger spots).

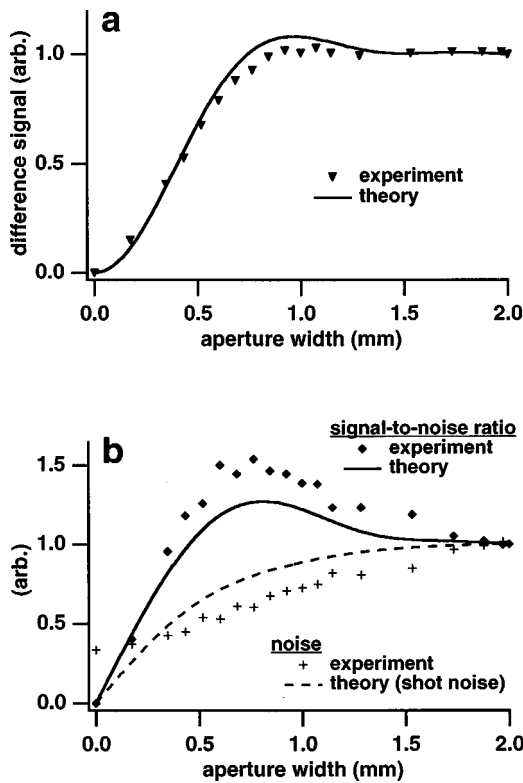


FIG. 4. (a) Experimental and theoretical detector difference signal as function of the aperture width for the 10 μm cantilever. The difference signal stays about constant for large aperture widths even though the aperture reduces the power of the incident beam. (b) Experimental and theoretical noise and signal-to-noise ratio as functions of the aperture width. The noise starts to drop as soon as incident beam power is lost. Therefore, the signal-to-noise ratio exhibits a maximum at a smaller than full aperture width.

is kept constant (Fig. 3). In this case, the difference signal decreases proportionally to the power on the detector.

The detection noise of the measurement could be defined as the rms value of the detector difference signal, $P_A - P_B$, in a bandwidth around the cantilever's resonance frequency (with the piezo actuator inactive). In that bandwidth, however, Brownian motion of the cantilever was dominant in the measured fluctuations. But Brownian motion of the cantilever is true cantilever motion and not detection noise. For the measurements presented here, Brownian motion of the cantilever remained below the detection noise level for frequencies below the resonance frequency and the detection noise level at those frequencies was flat. Therefore, we defined the detection noise in a measurement of a cantilever deflection as the rms value of the detector difference signal in a 50–90 kHz bandwidth. This rms value was measured indirectly by taking a power spectrum of the detector difference signal and integrating the spectrum from 50 to 90 kHz. The fact that the detection noise at those frequencies (including dc) is greater than the signal from cantilever movement supports the need for improved detection sensitivity.

The difference signal for the 10 μm cantilever is plotted versus aperture width [Fig. 4(a)]. When the aperture width is reduced, the difference signal stays about constant up to an aperture width of $a \approx 1.0$ mm, and then drops to 0 for a closed aperture ($a=0$ mm). The detection noise [Fig. 4(b)] starts to decrease right away and drops to an electronic back-

ground level at closed aperture. The signal-to-noise ratio [Fig. 4(b)] increases at first and peaks at $a \approx 0.7$ mm. Therefore, the signal-to-noise ratio of a measurement of the cantilever's deflection is higher at a reduced aperture width than it is at full aperture width. An even more dramatic effect was observed with a 40 μm cantilever [vibrated in air at its fundamental resonance frequency (147 kHz)]. The signal-to-noise ratio of a measurement of its vibration amplitude was recorded in a similar way as was done for the 10 μm cantilever (data not shown). The signal-to-noise ratio increased by a factor of almost 3 for a reduced aperture width.

III. THEORY

In this section we will first qualitatively explain why there is an optimum signal-to-noise ratio for an intermediate aperture width. We will then set up a theoretical model of the optical beam deflection detection in an AFM and derive expressions for the signal and for the noise of a measurement. Also, we will derive an expression for the minimum detectable cantilever deflection.

It is best to have a small spot on the detector: For a maximum difference signal, as much light as possible must shift from one detector segment toward the other when the cantilever is deflected. This can be achieved by accumulating most of the light power on the detector at its center, just between the two segments. In fact, all light power that is too far from the center of the detector such that it does not move from one segment to the other when the cantilever is deflected does not contribute to the difference signal.³⁰ The shot noise of the measurement, however, is proportional to the square root of the total light power on the detector, $P_A + P_B$. Therefore, all the light on the detector contributes to the shot noise but does not necessarily contribute to the difference signal. In our system (Fig. 1), the aperture plane and the detector plane are optically conjugated planes. When the cantilever is big enough to reflect the entire incident beam, then the aperture is imaged onto the detector, i.e., an identical image of the aperture is produced on the detector. Reducing the aperture width thus reduces the detector spot size and power, but does not change the irradiance at the center of the detector. Consequently, reducing the aperture width decreases the shot noise but does not decrease the difference signal. So the signal-to-noise ratio increases for reduced aperture width. Reducing the aperture width, however, also increases the focused spot size on the cantilever. At a certain aperture width, the focused spot on the cantilever becomes larger in size than the cantilever itself. Now, light spills over the cantilever's edges and the spot on the detector does not decrease much further in size, but only in power. The difference signal now decreases faster than the shot noise and so the signal-to-noise ratio decreases as well.

To quantitatively model this behavior, we refer to the experimental setup in Fig. 1. A collimated monochromatic laser beam passes through an aperture and is focused onto the cantilever by a converging lens. The light reflected from the cantilever is collimated again by the same lens and is directed onto the detector. For simplicity we keep the following analysis one-dimensional, i.e., we assume a one-dimen-

sional aperture and a one-dimensional cantilever. This is no limitation of the general case if we assume that the irradiance distribution of the laser light in the direction of the cantilever width can be factored out and all integrals in that dimension can be extended to infinity. The first condition is satisfied for the approximately Gaussian beam of a single-mode laser diode. The second condition is fulfilled when we assume that the spot widths on the cantilever and on the detector are smaller than the cantilever width and the detector width, respectively. Within those conditions, the particular size and shape of the focused spot in the direction along the cantilever width is not critical to the detection sensitivity (so only the size and shape along the cantilever length matters). This one-dimensional model is reasonable since we are interested in measuring the vertical deflection of the cantilever, i.e., how much the tip of the cantilever moves up and down. In case we wanted to measure lateral or torsional cantilever deflections, however, as is done in friction force microscopy, we would have to consider the dimension along the cantilever width as well.

We assume that the irradiance distribution of the incident beam in the plane of the aperture is of Gaussian shape:

$$I_i(x) = I_0 e^{-2(x/w)^2}, \tag{1}$$

where w is the collimated $1/e^2$ beam diameter and I_0 is a constant related to the total power of the incident (one-dimensional) beam, P_0 , by

$$I_0 = \sqrt{\frac{8}{\pi w^2}} P_0. \tag{2}$$

To perform the transformation of the irradiance profile of the beam as it passes through the optical system, we consider the scalar wave function³¹

$$E_i(x) = \sqrt{I_0} e^{-(x/w)^2}. \tag{3}$$

The scalar wave function is a function such that the square of its modulus is the irradiance. The lens focuses the part of the beam that passes through the aperture onto the cantilever and we calculate the focused spot profile $E_c(p)$ by the diffraction integral:^{31,32}

$$E_c(p) = \sqrt{\frac{\alpha_1 k}{2\pi f}} \int_{-a/2}^{a/2} dx E_i(x) e^{-ikpx/f}, \tag{4}$$

where $k = 2\pi/\lambda$ is the wave number of the incident beam, a is the aperture width, f is the focal length of the lens and α_1 is a loss factor ($0 \leq \alpha_1 \leq 1$) due to absorption and stray reflection of the light in the optical elements. We neglected vignetting effects due to the finite extent of the lens and assumed the aperture was located at the back focal plane of the lens by dropping a curvature phase factor. Mathematically, Eq. (4) constitutes a Fourier transform of the incident beam irradiance. Note that $E_c(p)$ is real, but generally not Gaussian. The focused spot is now moved on the cantilever to position p_c and the part of the incident beam that hits the cantilever is reflected back up, passes back through the lens, and is directed onto the detector. The spot profile on the detector can be approximated for small cantilever deflections ($z \ll \lambda$) by the diffraction integral

$$E_d(s) = \sqrt{\frac{\alpha_2 k}{2\pi f}} \int_0^L dp E_c(p - p_c) e^{2ikzh(p)} e^{-ikps/f}, \tag{5}$$

where p_c is the position of the center of the focused spot on the cantilever, z is the deflection of the cantilever at the tip ($p = L$ in our case) and $h(p)$ is the functional form of the shape of the cantilever, normalized to $h(0) = 0$ and $h(L) = 1$. α_2 is the loss factor ($0 \leq \alpha_2 \leq 1$) for the reflected beam, accounting for both the transmittance of the cantilever and for light power loss in the optical elements. The phase factor containing $h(p)$ accounts for phase shifts in the reflected light from different positions on the cantilever. It arises because light that is reflected from the cantilever base has to travel an additional distance $2z$ before it reaches the detector as compared to a similar reflection from the cantilever tip. Note that no assumptions are made about the particular normalized shape of the cantilever, $h(p)$.

The detector is sensitive to the irradiance of the light and the detector segments are collecting the light power

$$P_A = \int_0^b |E_d(s)|^2 ds \tag{6}$$

and

$$P_B = \int_{-b}^0 |E_d(s)|^2 ds. \tag{7}$$

At zero deflection of the cantilever, $z = 0$, the spot is centered on the detector and $P_A = P_B$. The size of each detector segment, b , should be chosen large enough such that the spot fits on the detector, which was the case for the experiment. Then the integrals in Eqs. (6) and (7) can be extended to infinity. We assume that the detector is ideal (perfect 100% responsivity and zero noise). Then the difference signal, S , of a measurement of the cantilever's deflection, z , is the difference of the incident powers onto the two detector segments:

$$\begin{aligned} S = P_A - P_B &\cong \left(\int_0^\infty - \int_{-\infty}^0 \right) ds |E_d(s)|^2 \\ &= \frac{k\alpha_2}{2\pi f} \left(\int_0^\infty - \int_{-\infty}^0 \right) ds \int_0^L dp \int_0^L dp' \\ &\quad \times E_c(p - p_c) E_c^*(p' - p_c) \\ &\quad \times e^{2ikz(h(p) - h(p'))} e^{-iks(p - p')/f} \\ &= \frac{\alpha_2}{i\pi} \mathcal{P} \int_0^L dp \int_0^L dp' E_c(p - p_c) \\ &\quad \times E_c^*(p' - p_c) \frac{e^{2ikz(h(p) - h(p'))}}{p - p'}. \end{aligned} \tag{8}$$

\mathcal{P} denotes the Cauchy principal part of the integral. The asterisk denotes the complex conjugate. For small cantilever deflections, $z \ll 1/k$, the exponential in the integrand can be approximated by a Taylor expansion with respect to z about $z = 0$,

$$e^{2ikz(h(p) - h(p'))} \cong 1 + 2ikz(h(p) - h(p')). \tag{9}$$

When inserting Eq. (9) into Eq. (8) and noting that E_c is real, the 0th-order term integrates out to 0 (since the integrand is antisymmetric with respect to p and p') and we obtain for the difference signal:

$$S = z \frac{4\alpha_2}{\lambda} \int_0^L dp \int_0^L dp' E_c(p-p_c) E_c(p'-p_c) \frac{h(p)-h(p')}{p-p'} \quad (10)$$

The \mathcal{P} denoting the Cauchy principal part was dropped since the integrand is no longer singular at $p=p'$. S is proportional to z and is inversely proportional to λ (i.e., small wavelengths are preferable for a good detection). We define the optical detection sensitivity, σ , for small cantilever deflections, z , as the rate with which the difference signal increases when the cantilever is deflected:

$$\sigma = \frac{S}{z} \quad (11)$$

A fundamental lower limit to the noise in a measurement of the cantilever deflection is set by the quantized nature of the light, which results in shot noise rms power fluctuations:

$$N = \sqrt{2\hbar\omega(P_A + P_B)\Delta f} \quad (12)$$

where $P_A + P_B$ is the total light power on the detector, $\hbar\omega$ is the energy of one photon and Δf is the detection bandwidth.

Finally, we define the signal-to-noise ratio (SNR) of a measurement of a small cantilever amplitude as the quotient of Eqs. (10) and (12),

$$\text{SNR} = \frac{S}{N} = \frac{\sigma}{N} z \quad (13)$$

The factor σ/N is the signal-to-noise ratio per unit cantilever deflection and directly represents the ‘‘goodness’’ of the optical detection. σ/N is independent of the particular cantilever deflection but depends on the cantilever shape. The minimum detectable cantilever deflection ($\text{SNR}=1$) is

$$z_{\min} = \frac{N}{\sigma} \quad (14)$$

There are three special cases of immediate interest for the cantilever shape, $h(p)$, in Eq. (10). The first case is that of a straight, rigid lever, hinged at its base, with a normalized shape

$$h_1(p) = \frac{p}{L} \quad (15)$$

In this case, the analysis of the optical lever sensitivity is simplest, since the cantilever acts like a flat mirror. This case was treated in the theory by Gustafsson and Clarke.²⁹

A more realistic atomic force microscope cantilever, however, is a flexible cantilever that is clamped at its base and free at its tip. If a static, vertical force acts on the tip, the cantilever will flex and have a slope that is largest at the tip and zero at the base. The shape of a statically curved cantilever is³³

$$h_2(p) = \frac{3Lp^2 - p^3}{2L^3} \quad (16)$$

This case is often applicable for force curve or contact mode operation. A third case applies for modes of operation where the cantilever is vibrated at its fundamental resonance frequency, for example in ac noncontact¹³ or tapping mode³⁴ operations. The shape of a cantilever vibrating at its fundamental resonance frequency is slightly different from that of a statically deflected cantilever and has the functional shape³³

$$h_3(p) = G(\cosh \kappa p - \cos \kappa p) + H(\sinh \kappa p - \sin \kappa p), \quad (17)$$

where $\kappa L = 1.8751$, $G = 0.5000$, and $H = -0.3670$. This is the functional form of the cantilever shape that we used in our theoretical calculations, since it most closely matched the experimental conditions.³⁵ For higher order vibrational modes of the cantilever, κL , G and H take on different values and the theoretical results would completely change. Generally a smaller spot would give maximum signal-to-noise ratio, because the region of maximum slope is smaller and because some parts of the cantilever have opposite slope and thus tend to cancel each other’s contribution to the difference signal.

The difference signal, the noise and the signal-to-noise ratio [Eqs. (10), (12) and (13)] were evaluated numerically³⁶ for different aperture widths, a , where we chose $f=6.75$ mm and $w=1.5$ mm to match the experimental parameter. For each aperture width, the position of the focused spot on the cantilever, p_c , was chosen by trial-and-error such that the difference signal calculated by Eq. (10) was maximized. This reflects our experimental procedure of maximizing the difference signal. This procedure also approximately maximizes the signal-to-noise ratio.

IV. DISCUSSION

The theoretical difference signal [Eq. (10)] of a deflection of the 10 μm cantilever is plotted versus the aperture width in Fig. 4(a) (both theoretical and experimental curves are normalized to 1 at $a=2.0$ mm). The theoretical difference signal closely matches the experimental data. The theoretical shot noise [Eq. (12)] and the signal-to-noise ratio using the shot noise [Eq. (13)] of a deflection of the 10 μm cantilever are plotted versus the aperture width in Fig. 4(b) (also normalized to 1 at $a=2.0$ mm). The theoretical signal-to-noise ratio first increases for decreasing aperture width and exhibits a peak at $a \cong 0.8$ mm. This optimum aperture width representing the best performance of the instrument closely predicts the experimentally determined optimum aperture width ($a \cong 0.7$ mm). The reason that the correspondence between theory and experiment in Fig. 4(b) is worse than in Fig. 4(a) is that the theoretical noise differs from the experimental noise. We had only considered the fundamentally limiting shot noise in the theory, which underestimates the total noise in the measurement. (The fact that the theoretical noise seems to overestimate the experimental noise at intermediate aperture widths is due to the normalization.) There are other noise sources that usually exceed the fundamental shot noise limit such as power or pointing fluctuations of the laser light or electrical noise of the detector.³³ The theoretical minimum detectable cantilever deflection in a

1 Hz detection bandwidth using our setup with the optimum aperture width for the 10 μm cantilever calculates to $z_{\text{min}} \cong 2.5 \times 10^{-15} \text{m}$ [Eq. (14), $\alpha_1 = \alpha_2 = 1$], but experimental values can be one order of magnitude higher.

The beneficial effect of the aperture increases with larger cantilevers. For example, the signal-to-noise ratio of a measurement of the deflection of a 40 μm cantilever could be increased by a factor of almost 3 at an intermediate aperture width.

Future improvements of the experimental setup could include the possibility to apodize the aperture to approximately preserve the Gaussian shape of the incident beam. This would avoid higher-order irradiance maxima of the beam in the cantilever plane that could miss the cantilever, be reflected up by the sample and interfere in a nonpreferred way with the light reflected off the cantilever. A more general improvement would be an aperture with a two-dimensional pattern whose transmittance varies across the aperture in order to produce a variety of different spot shapes on the cantilever. Another method to match the focused spot to the cantilever in length would be the use of an adjustable beam expander in place of the adjustable aperture. The adjustable beam expander could vary the incident beam diameter and thus match the focused spot to the cantilever in size without cutting out beneficial incident light power. Alternatively, removable and interchangeable focusing elements could be used. The above equations would still be valid with a slight modification of Eq. (4). With an adjustable beam expander, cantilevers of various sizes could be used at the same detection sensitivity.

V. CONCLUSION

We have used an adjustable aperture in the incident beam path of an AFM for small cantilevers. The adjustable aperture optimizes the detection sensitivity when using the AFM with different size cantilevers. Different cantilever sizes require different aperture widths for maximum detection sensitivity. The signal-to-noise ratio of the detection was increased by a factor of 1.5 to nearly 3 when using the aperture. We have set up a theoretical model explaining this behavior. This model is quite general and takes into account the particular functional shape of the cantilever when it is deflected. The results were derived for an AFM for small cantilevers, but can easily be applied for conventional AFMs with optical beam deflection detection.

ACKNOWLEDGMENTS

The authors thank Jason Cleveland, Roger Proksch, Deron Walters, Mario Viani, Kerem Yaman and Conrad Hirano for helpful discussions and Alexander Lobkovsky for checking the formulas. This work was supported by the National Science Foundation under Grant No. DMR-9622169 and by the U.S. Army Research Office under Grant No. DAAH04-96-1-0443. The authors also thank Digital Instruments for AFM support.

- ¹G. Binnig, C. F. Quate, and C. Gerber, *Phys. Rev. Lett.* **56**, 930 (1986).
- ²T. E. Schäffer, J. P. Cleveland, F. Ohnesorge, D. A. Walters, and P. K. Hansma, *J. Appl. Phys.* **80**, 3622 (1996).
- ³T. E. Schäffer, M. Viani, D. A. Walters, B. Drake, E. K. Runge, J. P. Cleveland, M. A. Wendman, and P. K. Hansma, *Proc. SPIE* **3009**, 48 (1997).
- ⁴M. Radmacher, M. Fritz, H. G. Hansma, and P. K. Hansma, *Science* **265**, 1577 (1994).
- ⁵M. Rief, M. Gautel, F. Oesterhelt, J. M. Fernandez, and H. E. Gaub, *Science* **276**, 1109 (1997).
- ⁶D. A. Walters, J. P. Cleveland, N. H. Thomson, P. K. Hansma, M. A. Wendman, G. Gurley, and V. Elings, *Rev. Sci. Instrum.* **67**, 3583 (1996).
- ⁷D. A. Walters, M. Viani, G. T. Paloczi, T. E. Schäffer, J. P. Cleveland, M. A. Wendman, G. Gurley, V. Elings, and P. K. Hansma, *Proc. SPIE* **3009**, 43 (1997).
- ⁸R. Berger, E. Delamarche, H. P. Lang, C. Gerber, J. K. Gimzewski, E. Meyer, and H. J. Güntherodt, *Science* **276**, 2021 (1997).
- ⁹F. Ohnesorge and G. Binnig, *Science* **260**, 1451 (1993).
- ¹⁰J. P. Cleveland, T. E. Schäffer, and P. K. Hansma, *Phys. Rev. B* **52**, R8692 (1995).
- ¹¹G. Meyer and N. M. Amer, *Appl. Phys. Lett.* **53**, 1045 (1988).
- ¹²S. Alexander, L. Hellems, and O. Marti, J. Schneir, V. Elings, P. K. Hansma, M. Longmire, and J. Gurley, *J. Appl. Phys.* **65**, 164 (1989).
- ¹³Y. Martin, C. C. Williams, and H. K. Wickramasinghe, *J. Appl. Phys.* **61**, 4723 (1989).
- ¹⁴D. Sarid, D. A. Iams, V. Weissenberger, and L. S. Bell, *Opt. Lett.* **13**, 1057 (1988).
- ¹⁵D. Rugar, H. J. Mamin, and P. Guethner, *Appl. Phys. Lett.* **55**, 2588 (1989).
- ¹⁶C. Schönenberger and S. F. Alvarado, *Rev. Sci. Instrum.* **60**, 3131 (1989).
- ¹⁷G. Neubauer, S. R. Cohen, G. M. McClelland, D. Horne, and C. M. Mate, *Rev. Sci. Instrum.* **61**, 2296 (1990).
- ¹⁸M. Tortonese, H. Yamada, R. C. Barret, and C. F. Quate, in *The Proceedings of Transducers '91* (IEEE, New York, 1991), p. 448.
- ¹⁹S. C. Minne, S. R. Manalis, and C. F. Quate, *Appl. Phys. Lett.* **67**, 3918 (1995).
- ²⁰B. Drake, C. B. Prater, A. L. Weisenhorn, S. A. Gould, T. R. Albrecht, C. F. Quate, D. S. Cannell, H. G. Hansma, and P. K. Hansma, *Science* **243**, 1586 (1989).
- ²¹Digital Instruments, Santa Barbara, California.
- ²²Park Scientific Instruments, Sunnyvale, California.
- ²³T. R. Albrecht, S. Akamine, T. E. Carver, and C. F. Quate, *J. Vac. Sci. Technol. A* **8**, 3386 (1990).
- ²⁴J. E. Sader, *Rev. Sci. Instrum.* **66**, 4583 (1995).
- ²⁵W. Kulisch, A. Malave, G. Lippold, W. Scholz, C. Mihalcea, and E. Oesterschulze, *Diamond Relat. Mater.* **6**, 906 (1997).
- ²⁶R. Pechmann, J. M. Kohler, W. Fritzsche, A. Schaper, and T. M. Jovin, *Rev. Sci. Instrum.* **65**, 3702 (1994).
- ²⁷M. B. Viani, A. Chand, and P. K. Hansma (unpublished).
- ²⁸C. A. J. Putman, B. G. De Grooth, N. F. Van Hulst, and J. Greve, *J. Appl. Phys.* **72**, 6 (1992).
- ²⁹M. G. L. Gustafsson and J. Clarke, *J. Appl. Phys.* **76**, 172 (1994).
- ³⁰It is necessary, however, that the spot fits on the detector.
- ³¹M. Born and E. Wolf, *Principles of Optics* (Pergamon, Oxford, 1980).
- ³²J. W. Goodman, *Introduction to Fourier Optics* (McGraw-Hill, San Francisco, CA, 1968).
- ³³D. Sarid, *Scanning Force Microscopy: With Applications to Electric, Magnetic, and Atomic Forces*, 2nd ed. (Oxford University Press, New York, 1994).
- ³⁴Q. Zhong, D. Inniss, K. Kjoller, and V. B. Elings, *Surf. Sci.* **290**, L688 (1993).
- ³⁵U. Rabe, K. Janser, and W. Arnold, *Rev. Sci. Instrum.* **67**, 3281 (1996).
- ³⁶MATHEMATICA 3.0 (Wolfram Research, Champaign, IL); W. H. Press, B. P. Flannery, S. A. Teukolski, and W. T. Vetterling, *Numerical Recipes in C*, 2nd ed. (Cambridge University Press, Cambridge, 1992).